Published in final edited form as:
J Mol Cell Cardiol. 2012 November ; 53(5): 626–638. doi:10.1016/j.yjmcc.2012.08.002.

Collagen XIV is important for growth and structural integrity of the myocardium

Ge Tao, PhD[a,b], **Agata K. Levay, MS**[c], **Jacqueline D. Peacock, PhD**[c], **Danielle J. Huk, BS**[b,c], **Sarah N. Both**[b], **Nicole H. Purcell, PhD**[d], **Jose R. Pinto, PhD**[c,e], **Maarten L. Galantowicz, BS**[b], **Manuel Koch, PhD**[f], **Pamela A. Lucchesi, PhD**[b,g], **David E. Birk, PhD**[h], and **Joy Lincoln, PhD**[b,g,†]

[a]Molecular, Cell and Developmental Biology Graduate Program, Leonard M. Miller School of Medicine, P.O. Box 016960 (R-124), Miami, Florida, 33101, USA

[b]Center for Cardiovascular and Pulmonary Research, The Research Institute at Nationwide Children's Hospital, 700 Children's Drive, Columbus, Ohio, 43205, USA

[c]Department of Molecular and Cellular Pharmacology, Leonard M. Miller School of Medicine, P.O. Box 016430 (R-189), Miami, Florida, 33101, USA

[d]Department of Pharmacology, University of California, San Diego, 9500 Gilman Drive, La Jolla, California, 92093-0636, USA

[e]Department of Biomedical Sciences, College of Medicine, Florida State University, Tallahassee, Florida, 32308, USA

[f]Center for Biochemistry, Medical Faculty, University of Cologne, D-50931 Cologne, Germany

[g]Department of Pediatrics, The Ohio State University, Columbus, Ohio, USA

[h]Department of Molecular Pharmacology & Physiology, University of South Florida, Morsani College of Medicine, 12901 Bruce B. Downs Blvd., Tampa, Florida, 33612, USA

Abstract

Collagen XIV is a fibril-associated collagen with an interrupted triple helix (FACIT). Previous studies have shown that this collagen type regulates early stages of fibrillogenesis in connective tissues of high mechanical demand. Mice null for Collagen XIV are viable, however formation of the interstitial collagen network is defective in tendons and skin leading to reduced biomechanical function. The assembly of a tightly regulated collagen network is also required in the heart, not only for structural support but also for controlling cellular processes. Collagen XIV is highly expressed in the embryonic heart, notably within the cardiac interstitium of the developing myocardium, however its role has not been elucidated. To test this, we examined cardiac phenotypes in embryonic and adult mice devoid of Collagen XIV. From as early as E11.5, *Col14a1*$^{-/-}$ mice exhibit significant perturbations in mRNA levels of many other collagen types and remodeling enzymes (MMPs, TIMPs) within the ventricular myocardium. By post natal

†Corresponding author: The Research Institute at Nationwide Children's Hospital, 700 Children's Drive, W309, Columbus, OH, 43205, +1-614-722-3330 (fax), +1-614-722-5152 (phone), joy.lincoln@nationwidechildrens.org.

Disclosures. The authors of this paper have nothing to disclose.

Conflict of Interest. The authors of this paper have no conflicts of interest.

stages, collagen fibril organization is in disarray and the adult heart displays defects in ventricular morphogenesis. In addition to the extracellular matrix, *Col14a1*$^{-/-}$ mice exhibit increased cardiomyocyte proliferation at post natal, but not E11.5 stages, leading to increased cell number, yet cell size is decreased by 3 months of age. In contrast to myocytes, the number of cardiac fibroblasts is reduced after birth associated with increased apoptosis. As a result of these molecular and cellular changes during embryonic development and post natal maturation, cardiac function is diminished in *Col14a1*$^{-/-}$ mice from 3 months of age; associated with dilation in the absence of hypertrophy, and reduced ejection fraction. Further, *Col14a1* deficiency leads to a greater increase in left ventricular wall thickening in response to pathological pressure overload compared to wild type animals. Collectively, these studies identify a new role for type XIV collagen in the formation of the cardiac interstitium during embryonic development, and highlight the importance of the collagen network for myocardial cell survival, and function of the working myocardium after birth.

Keywords

Collagen XIV; Myocardium; Extracellular Matrix; Cardiomyocytes; Cardiac fibroblasts

1. Introduction

The working heart requires integration of many diversified structures including the myocardium, valves and vessels. To achieve this, each structure is composed of specialized cell populations and a specific extracellular matrix (ECM) network that collectively provide the necessary biomechanics to meet hemodynamic demands during the cardiac cycle [1]. In the myocardium, cardiac myocytes and fibroblasts are the predominant cell types arranged within a complex ‘cardiac interstitium’ primarily composed of collagens, proteoglycans and glycoproteins [2]. During cardiogenesis, the ECM plays a crucial role in regulating many cellular processes including proliferation, adhesion, migration and changes in gene expression [1, 3, 4]. Further, perturbation of genes encoding matrix proteins can result in prenatal lethality or congenital heart disease in humans [1, 3]. After birth, the ECM is required to maintain homeostasis of adult cardiac structures under normal physiological conditions and in response to stress or injury [1, 3]. This is achieved through remodeling that commonly occurs in the myocardium following injury, such as myocardial infarction. This process is characterized by cardiac fibroblast activation to increase ECM synthesis and deposition of scar tissue to replace necrotic cardiomyocytes and maintain structural integrity [5]. While short-term remodeling can be beneficial, persistent ECM deposition after repair is deleterious and leads to ventricular stiffening and congestive heart failure [5]. Therefore it is imperative that the myocardium establishes and maintains an appropriately organized ECM network to meet the functional demands of healthy and compromised hearts.

Like most connective tissue systems, the development and maintenance of the cardiac interstitium is dependent on the assembly of collagen fibrils, predominantly types I, III and V, and the subsequent organization into highly ordered fibers [2, 6]. This hierarchical organization of collagen fibrils is essential for providing tensile strength to the myocardium in response to changes in hemodynamic load, and functions to transmit force during the cardiac cycle. The process of fiber formation from fibril bundles requires two major groups of fibril-associated molecules; the first are members of the leucine-rich repeat family of proteoglycans and glycoproteins including decorin, lumican, biglycan and fibromodulin [7–10]. The second group is the fibril-associated collagens with interrupted triple helices (FACIT) that include Collagen XIV, previously shown to be highly expressed in areas of high mechanical stress [11–15]. In its role as a FACIT, Collagen XIV predominantly interacts with, and adheres to Collagen I to promote fiber assembly [16]. Mice null for

Collagen XIV are viable but detailed analyses of skin and tendons reveal defects in fibril growth and fiber assembly during embryonic development [11]. As a result of altered fibrillogenesis, fiber structure is compromised and the biomechanical functions of these tissues are significantly diminished [11]. Therefore suggesting that Collagen XIV is important for ECM assembly and tissue function in tendons and skin.

To date, there are limited studies examining the requirement of collagens for structure and function of the heart. A recent study reported that Collagen XV, a non-fibrillar collagen type localized to basement membranes of microvessels and cardiac myocytes, is necessary for organization of the cardiac interstitium and vasculature [17]. As a result, cardiomyocyte size is reduced and alignment is disrupted in young *Col15a1*$^{-/-}$ mice, while older animals develop early onset cardiomyopathy [17]. In addition to this study, we have described the roles of fibrillar Collagens V and XI for myocardial morphogenesis and formation of the cardiac valves during embryonic development [18]. In another study from our group, we reported Collagen XIV expression in the heart [19, 20], however its function was not examined. Therefore, in this current study we set out to characterize the cardiovascular phenotypes of embryonic and adult hearts from *Col14a1*$^{-/-}$ mice [11] at molecular, cellular and functional levels. Our data show that Collagen XIV plays an important role in establishing the cardiac interstitium within the developing myocardium, in addition to regulating cardiomyocyte growth and cardiac fibroblast survival. These alterations during embryonic development lead to functional defects in adult mice and greater increases in chamber wall growth in the absence of hyperplasia, in *Col14a1*$^{-/-}$ hearts following pressure overload conditions. Collectively our findings reveal previously unappreciated roles for FACIT collagens in the formation of the cardiac interstitium and development of the mature myocardium.

2. Material and methods

2.1 Generation of mice

Collagen (Col) 14a1$^{+/-}$ mice [11] were inbred to generate *Col14a1*$^{-/-}$ and wild type (*Col14a1*$^{+/+}$) controls. Genotyping by PCR was performed as previously described [11] using genomic DNA isolated from mouse tail biopsies. All animal procedures were approved and performed in accordance with IACUC institutional guidelines at The Research Institute at Nationwide Children's Hospital.

2.2 Histology

Whole hearts from *Col14a1*$^{-/-}$ and *wild type* (*Col14a1*$^{+/+}$) mice were collected at E11.5, E14.5, Post natal day 1 (PND1) and 3 months of age in 1X Phosphate Buffered Saline (PBS) and either fixed in 4% paraformaldehyde (PFA) overnight at 4°C or left unfixed. Fixed tissues were subsequently processed for either paraffin- or cryo-embedding and sectioned at 6 μm and 10 μm, respectively. Alternatively, unfixed tissue was immediately processed for frozen block cryo-embedding and 10 μm tissue sections were cut. For fluorescent immunohistochemistry, fixed tissue sections were processed as previously described [21], followed by an overnight incubation at 4°C with primary antibodies against Collagen XIV [22] (1:200), Vimentin (Abcam, 1:200) Laminin a-2 (Sigma, 1:200), N-cadherin (Invitrogen, 1:200), MF20 (Hybridoma Bank, 1:400) and Phospho-histone H3 (Millipore, 1:200). Unfixed frozen sections were post fixed in ice-cold acetone at −20 °C for 15 mins, blocked in 5% bovine serum albumin/1XPBS for 30 mins and incubated with anti- Collagen Ia1 (Abcam, 1:200), Laminin a2 (Sigma, 1:200), MF20 (Hybridoma Bank, 1:400), Cleaved Caspase-3 (Cell Signaling, 1:200) and Thy-1 (BD Pharmingen, 1:100) for 2 hours at room temperature. Detection of primary antibodies was performed using appropriate conjugated secondary antibodies (1:200, PBS) (Alexa-Fluor, Invitrogen). Nuclei were detected by

staining with DAPI (1μg/ml, 10 minutes) and/or cell membranes with Wheat Germ Agglutinin (WGA) (10μg/ml, 10 minutes). Stained tissue was mounted in Vectashield Hard Set mounting medium (Vector Laboratories). Images were captured using an Olympus BX51 fluorescent microscope. Quantitation of cardiac fibroblast and cardiomyocyte number was determined by counting cells the number of $Thy1^+/Vimentin^+$ (fibroblasts) or $MF20^+$ (cardiomyocytes) cells, over the total number of DAPI-stained nuclei. To further examine proliferation and apoptosis rates of these cells, the number of $Thy1^+$ (fibroblasts) or $MF20^+$ double stained with Phospho-Histone $H3^+$ (proliferation) or Cleaved Caspase-3 (apoptosis) were reported over the number of nuclei in at least 10 microscopic images from 3 hearts. The average number of cardiomyocytes (outlined by WGA staining), and number and length of intercalated discs (labeled by antibody against N-cadherin) were determined using Photoshop CS5 software (Adobe) (10 fields, n=3). Trichrome and Pentachrome staining were performed on paraffin tissue sections from *Col14a1*$^{-/-}$ and *wild type* adult hearts as previously reported [19]. Quantification of fibrosis in Trichrome stained tissue sections was determined by counting the total pixel numbers of blue area (total collagens) normalized to red area (cardiac muscle) using ImagePro Plus software. Significant differences in *Col14a1*$^{-/-}$ compared to *wild types* was determined using Student's *t*-test ($p<0.05$).

2.3 Transmission Electron Microscopy

Ventricles were isolated from 3 month old *Col14a1*$^{-/-}$ and *wild type* mice and processed for transmission electron microscopy as described [23] [11]. Briefly, left ventricles were dissected and fixed in 4% PFA, 2.5% glytaraldehyde, 0.1 M sodium cacodylate, pH7.4, with 8.0 mM $CaCl_2$, post-fixed with 1 % osmiumtetroxide and En-Bloc-Stained with uranyl acetate/50% ethanol. After dehydration in an ethanol series, followed by propylene oxide, tissue samples were infiltrated and embedded in a mixture of Embed 812, nadic methyl anhydride, dodecenyl succinic anhydride, and DMP-30 (Electron Microscopy Sciences, Hatfield, PA). Thin sections (90nm) were cut using a Leica Ultracut UCT ultramicrotome and post-stained with 2% aqueous uranyl acetate and 1% phosphotungstic acid, pH3.2. Sections were examined at 80 kV using JEOL 1400 transmission electron microscope and captured with a Gatan Ultrascan US1000 2 K digital camera.

2.4 Western blot

Collagens were extracted from *Col14a1*$^{-/-}$ and *wild type* ventricles at PND1 as previously described [11] using a 1X buffer (20 mM Tris (pH7.5), 150mM NaCl, 1mM EDTA, 1mM EGTA, 1% Triton X-100, 2.5mM sodium pyrophosphate, 1mM β-glycerophosphate, 1mM Na_3VO_4, supplemented with Complete EDTA (Roche) free protease inhibitor cocktail). 30μg of extracted collagen was run on a pre-cast 8% SDS PAGE gel (Invitrogen) and transferred to nitrocellulose membranes as described [19]. Membranes were blocked in 5% fat free dried milk for 1 hour and probed with antibodies against Collagen XIV [22] (1:1000, 2 hours) and Actin (1:5000, 1 hour, Chemicon/Millipore), followed by incubation with anti-mouse horseradish peroxidase-conjugated secondary antibody (1:15000, 1 hour, Cell signaling). Membranes were then washed three times in 1X TBST for 15 minutes. Western blots were developed using Super Signal West Pico Substrate (Pierce) and BioMax MR film (Eastman Kodak).

2.5 PCR analyses

Total mRNA was isolated from *Col14a1*$^{-/-}$ and *wild type* ventricles at E11.5, PND1 and 3 months of age, as well as TAC and Sham-operated mice using TRIzol [24]. 200~400 ng mRNA was used to generate cDNA using the high-capacity cDNA kit (Applied Biosystems) [21]. 1 μg of cDNA from each mRNA sample was subject to custom Taqman Low Density Array (TLDA) analysis using the 7900 HT Fast Real-Time System according the manufacturer's instructions (Applied Biosystems). The ΔCt (cycle count) of each target

gene was determined by normalization to the Ct of *18s*. Fold changes in *Col14a1*$^{-/-}$ samples over wild types were determined as described [19]. Alternatively cDNA from E11.5, PN and 3 month old *Col14a1*$^{-/-}$ and *wild type* ventricles was subject to quantitative PCR (qPCR) using Taqman probes (Applied Biosystems) against mouse *Col14a1* and normalized to *18s* expression level (n=3). For absolute transcript calculation, the formula $\mathrm{POWER}^{(2,\,((40-\Delta Ct)+Ct\,18s)}$ was used, with Ct*18s* denoting the average cycle count of *18s* mRNA levels. In addition, qPCR was also performed with cDNA prepared from TAC and Sham-operated (see below) *Col14a1*$^{-/-}$ and *wild type* ventricle CDNA using specific primers targeting mouse *Col1a1* (Forward: GAGCGGAGAGTACTGGATCG; Reverse GTTCGGGCTGATGTACCAGT), *Col3a1* (Forward: ACCAAAAGGTGATGCTGGAC; Reverse: GACCTCGTGCTCCAGTTAGC), *Lox* (Forward: TACTCCAGACTCTGTGCGCT; Reverse: GGACTCAGATCCCACGAAGG), *Plod1* (Forward: TTCGTCGTCCGCTATAAGCC; Reverse: AGGAAGCCCCTCGTGATAGT), *Plod2* (Forward: GAGCACTGAGTCCTGATGGG; Reverse: TGTTTCCGGAGTAGGGGAGT), *P3H1* (Forward: CGCTTACACCTTTCGGGACT; Reverse: GTATCCGCTCCAGTTCTCGG), *Glt25D1* (Forward: CATGTGCTTGCCTGGGACTA; Reverse: TCTCTTGGTGGTCAGCCCTA) and *Glt25D2* (Forward: ATGTCAGGTGCAATGCTGGA; Reverse: CACAAGCTGGGGCTGGATAA), normalized to *L7* (Forward: GAAGCTCATCTATGAGAAGGC; Reverse: AAGACGAAGGAGCTGCAGAAC) and detected using Sybr Green as described [19]. Statistical significance in transcript levels between *Col14a1*$^{-/-}$ and *wild type* samples were determined using Student's *t*-test on at least 3 independent experiments with $p<0.05$.

2.6 Skinned Fiber Assays

Mouse Skinned Cardiac Fiber Preparation—Skinned papillary muscles were prepared from left ventricles isolated from *Col14a1*$^{-/-}$ and *wild type* mice (>n=3) at 3 months of age. Small bundles of fibers were isolated and treated overnight with a *p*Ca 8.0 relaxing solution (10^{-8} M $[Ca^{2+}]_{free}$, 1 mM $[Mg^{2+}]_{free}$, 7 mM EGTA, 2.5 mM $MgATP^{2-}$, 20 mM MOPS, pH 7.0, 20 mM creatine phosphate, and 15 units/ml creatine phosphokinase) containing 1% Triton X-100 and including 50% glycerol at −20 °C. Fibers were then transferred to a similar solution without Triton X-100 and stored at ⁻20 °C [25].

Stretch-force Relationship Measurements at Low Ca^{2+} Concentration—Ventricular papillary muscle skinned fiber, prepared from 3 month old *Col14a1*$^{-/-}$ and *wild types* were mounted as described above. Fibers were treated with *p*Ca8.0 containing 1% Triton X-100 for 30 mins and extensively washed with *p*Ca 8.0 without Triton X-100. After the skinning process, the slack length from the fiber was determined by releasing and stretching until it starts to generate tension. This point was set as zero for both passive force and starting length. After this, the fiber was consecutively stretched 10% of its original length and the passive force in KN/m2 was recorded. These experiments were carried out at *p*Ca 8.0.

2.7 Echocardiography

Transthoracic encocardiography was performed on 3, 6 and 12 month old *Col14a1*$^{-/-}$ and *wild type* male mice, as well as the TAC and Sham-operated mice before and 2 weeks after the surgery, using the VisualSonics 770 system (Toronto, Canada) as described [21]. Mice were anesthetized by 1% isoflurane inhalation and placed on a heated platform (37°C). Two-dimensional imaging was recorded with a 45 MHz transducer to capture long- and short-axis projections with guided M-Mode, B-Mode and PW Doppler recorded. For data presented in Table 1, the average reading for each echocardiographic parameter was recorded from at least 3 distinct frames from n=5–8 individual mice from the four experimental groups (*wild type* Sham (n=6), *wild type* TAC (n=8), *Col14a1*$^{-/-}$ Sham (n=5), *Col14a1*$^{-/-}$ TAC (n=7))

both prior to surgery and two weeks post surgery. Statistical significance was determined using Student's t-test ($p<0.05$).

2.8 Transverse aortic constriction (TAC)

Artificial left ventricular pressure overload was performed on 8 week old *Col14a1*$^{-/-}$ and *wild type* mice following echocardiography, as previously described [26] with the modification of TAC and Sham-operated mice receiving Buprenorphine treatment subcutaneously (0.1 mg/kg) 12 hours after surgery. 2 weeks post surgery, mice were weighed and subjected again to echocardiography and then euthanized, hearts weighed and collected for analyses as described above.

2.9 Primary mouse cardiomyocyte isolation

Ventricular cardiomyocytes were isolated from 10 week old *Col14a1*$^{-/-}$ and *wild type* hearts (n=3) as described [27]. Briefly, each heart was mounted on a Langendorf apparatus followed by retrograde perfusion through the aorta with perfusion buffer (Alliance for Cell Signaling, Protocol PP00000125) [27] for 4 mins, followed by perfusion with buffer containing 12.5 μM $CaCl_2$, 0.14 mg/mL trypsin and 4 *Wünsch* units of Liberase TH (Roche) for 4 mins (*Col14a1*$^{-/-}$) or 6 mins (*wild type*). Ventricles were separated from the digested hearts, minced, triturated and cardiomyocytes were mechanically dispersed in perfusion buffer (containing 12.5 μM $CaCl_2$ and 10% calf serum), and filtered. The isolated cardiomyocytes were then resuspended in increasing concentrations of $CaCl_2$ over 16 mins to achieve a final concentration of 1 mM. Treated myocytes were plated on Laminin-coated 2-well chamber slides (Thermo) in Minimal Essential Medium with Hanks' salts and 2 mM L-glutamine (MEM), supplemented with 5% calf serum, 10mM 2,3-butanedione monoxime, and 100 U/mL penicillin-streptomycin. After 1-hour incubation (5% CO_2, 37 °C), plated cardiomyocytes were fixed with 2% PFA for 30 mins on ice and subjected to immunofluorescence using an antibody against MF20 (hybridoma bank, 1:400). Detection of the primary antibody against MF20 using appropriate secondary antibodies (Alexa-Fluor, Invitrogen) was performed and cells were further stained with WGA and DAPI as described above. Images of cells (400X magnification) were taken using Olympus BX51 microscope. The average size of each cardiomyocyte was determined by measuring the area (WGA^+) of 50–100 cells (n=3) using Image J software. Statistical significance in cardiomyocyte area in *Col14a1*$^{-/-}$ versus *wild type* mice was determined using Student's t-test (n=3, $p<0.05$).

3. Results

3.1 Collagen XIV is expressed in the developing heart

Collagen XIV is predominantly expressed in tissues of high mechanical stress [11–14], however its expression in the heart has not been fully examined. Using immunohistochemistry, Collagen XIV was not detected in the heart until embryonic day (E) 12.5 where it was observed in the developing epicardium and endocardial cushions (data not shown). By E14.5, expression was detectable at low levels within the interstitial space of the developing ventricular myocardium and epicardium (Figure 1A). In contrast, high levels of expression were observed in the developing rib structures (Figure 1A). By post natal (PN) stages, expression was higher within the subepicardial region (arrowhead, Figures 1B, E) as well as the interstitial space within the ventricular myocardium, particularly within the compact layer compared to the trabeculae layer (arrows, Figure 1B, E). Additional immunoreactivity was also seen within the developing valve leaflets and chordae tendineae (Figure 1C), as well as around the intramyocardial coronary vessels (Figure 1D). Expression was maintained in the adult myocardium (Figure 1F) and valve structures, although levels were less than during post natal stages (Figure 1F).

3.2 *Col14a1*$^{-/-}$ mice have attenuated cardiac function, but no change in the stretch-force relationship of the myocardium

To determine the role of Collagen XIV in the developing heart, cardiac structure and function was examined in *Col14a1*$^{-/-}$ and *Col14a1*$^{+/+}$ (*wild type*) mice [11]. Western blot analysis performed on collagen extracts from post natal mice confirms a knockout of Collagen XIV in *Col14a1*$^{-/-}$ hearts compared to wild types (Figure 2A). Histological examination of hearts from 3 month old *Col14a1*$^{-/-}$ mice revealed a 'rounded' ventricular chamber (Figure 2C) compared to littermate *wild types* (Figure 2B), with no gross changes in wall thickness; consistent with indifferent heart weight to body weight ratios at baseline (data not shown). At the functional level, echocardiography of 3, 6 and 12 month old *Col14a1*$^{-/-}$ males showed increased left ventricular end-diastolic volume at 12 months of age (110μl±6.7 vs. 88μl±9.4), and all time points examined during systole (50μl±3.77 vs. 35μl±4.6, 42μl±1.8 vs. 34μl±1.0, 59μl±4.1 vs. 40μl±5.8) (Figures 3A, B). In addition, ejection fraction was significantly decreased in mutant mice at 3 (50.6%±3.0 vs. 57%±2.8), 6 (49.4%±1.44 vs. 56.3%±0.9) and 12 months (47.6%±1.6 vs. 54.4%±2.2) (Figure 3E). In support of histological analyses, left ventricular posterior wall (LVPW) thickness was not significantly altered in mutant mice (Figures 3C, D), other than a subtle decrease in LVPW during systole at 12 months of age (0.91mm±0.05 vs. 1.12mm±0.07) (Figure 3D). To determine if Collagen XIV deficiency affects the biomechanics of the ventricular chamber, stretch-force relationship assays were performed using skinned papillary muscles isolated from 3 month old *Col14a1*$^{-/-}$ and *wild type* mice. Unlike previous studies in the skin in which the maximum stretch of skin was dramatically reduced [11], the resistance of ventricular skinned fibers to stretch (0–40%) under resting conditions was not altered in *Col14a1*$^{-/-}$ mice. Collectively, these data suggest that gross cardiac structure and myocardial contractility is modestly altered in *Col14a1*$^{-/-}$ mice.

3.3 Loss of Collagen XIV during embryogenesis disrupts extracellular matrix homeostasis within the developing and mature myocardial interstitium

To ascertain changes in the composition and organization of ECM components within the ventricular myocardium of *Col14a1*$^{-/-}$ mice, a combination of gene expression, immunohistochemistry and electron microscopy assays were performed. Using Taqman Low Density Array assays, the approximate transcript levels of *Col14a1* and several other collagen types were determined in ventricular tissue isolated from *wild type* and *Col14a1*$^{-/-}$ mice at E11.5, post natal and 3 months of age (Figure 4). In *wild type* mice, *Col14a1* mRNA levels were relatively high and comparable with *Col1a1* in the ventricular myocardium at E11.5 through post natal stages, while levels were significantly lower by 3 months of age. In the absence of Collagen XIV notable changes in mRNA levels of other collagen isoforms were observed in the ventricular myocardium of *Col14a1*$^{-/-}$ mice by E11.5. These include significant increases in *Col1a1, Col1a2, Col3a1, Col27a1* and *Col12a1* mRNA levels, and reduced *Col6a1* and *Col9a1*. At post natal stages, only *Col6a1* was affected with increased levels observed in null animals. By 3 months of age, levels of collagen isoforms were altered again in *Col14a1*$^{-/-}$ mice with alpha chain transcripts for fibril-forming collagen types *Col1a1, Col1a2, Col11a1, Col27a1* all increasing, along with the network collagen type, *Col8a2*, while levels of *Col12a1* (FACIT) were reduced. Consistent with a trend towards reduced levels of *Col1a1* in the ventricular myocardium at 3 months of age (Figure 4A), additional Western blot analysis showed a 2.6-fold and 2185-fold decrease in protein expression in ventricles from *Col14a1*$^{+/-}$ and *Col14a1*$^{-/-}$ mice, respectively (Figure 5A). In support, immunostaining revealed a similar trend within the epicardium and ventricular interstitium (Figure 5A). Collectively these data show that loss of Collagen XIV from early stages of embryogenesis alters mRNA levels of several other collagen types in the developing and mature ventricular myocardium.

To examine if changes in collagen transcripts are associated with alterations in overall collagen processing and myocardial matrix remodeling [28], qPCR analyses were performed. Compared to *wild types,* expression of *Plod1* that encodes the enzyme lysyl hydroxylase1, and *GLT25D1* and *GLT25D2* (procollagen galactosyltransferases) were increased in the ventricular myocardium of post natal *Col14a1*$^{-/-}$ mice (Figure 5B). Therefore suggesting that post translational modifications of collagens are affected in these mice. At the level of matrix remodeling, *Mmp2* (8.0±1.5), *Mmp9* (412±42.6), and their inhibitors *Timp2* (3.5±0.2) and *Timp3* (2.2±0.08) were increased in *Col14a1*$^{-/-}$ mice at E11.5. *Mmp2 and Mmp9* are gelatinases and serve to digest denatured collagens and Collagens IV and V within basement membranes [29]. In contrast, by post natal stages, *Mmp3*, known to target non-fibrillar collagens, proteoglycans, laminin, fibronectin and elastin, was significantly downregulated (0.0004±0.0002). However in the adult, only *Timp2* expression is decreased (0.3±0.09) (Figure 5C). Electron microscopy analysis revealed that these collective alterations in collagen and remodeling gene profiles have detrimental effects on the ultrastructure of the ventricular myocardium at post natal stages (Figure 5D–F). In *wild types*, collagen fibrils were highly organized and arranged in tight bundles within the interstitial space (Figure 5D), while in *Col14a1*$^{-/-}$ mice fibrils were abnormally dispersed throughout the interstitial space (Figures 5E–F). These observations suggest that Collagen XIV is required to establish and maintain a balanced and organized ECM environment in the development myocardium.

3.4 Myocyte cell size and number is altered in the post natal ventricular myocardium of *Col14a1*$^{-/-}$ mice

To determine potential changes in cardiomyocyte maturation and growth in *Col14a1*$^{-/-}$ mice, morphometric and proliferation analyses were performed. At E11.5, analysis of Phospho-histone H_3 (pHH_3) immunoreactivity revealed undetectable differences in cell proliferation in the ventricle of *Col14a1*$^{-/-}$ mice compared to *wild types* (Figure 6C). At this time, cardiomyocyte size was also comparable with wild type mice (data not shown). By post natal stages (PND1), proliferation rates of cells almost certainly cardiomyocytes (MF20-positive) was significantly higher in *Col14a1*$^{-/-}$ mice (7.2±0.19 vs. 3.6±0.4) (Figures 6A–C), however at 3 months levels were back comparable with *wild types*. Although no change in cell proliferation was observed at 3 months, changes in cardiomyocyte size and number were noted. N-cadherin immunostaining revealed dramatic increases in the number (57.3±1.78 vs. 38.7±1.2, per microscopic field) (Figure 6D–F), and length (2.69mm±0.17 vs. 9.24mm±0.5) (data not shown) of cardiomyocyte intercalated discs in *Col14a1*$^{-/-}$ mice compared to *wild types*, suggesting increased numbers of smaller cells. In support, cultured cardiomyocytes isolated from 10 week old *Col14a1*$^{-/-}$ mice are 24% (±0.04%) smaller than wild types (Figure 6G–I). Although it is noted that this in vitro approach is circumstantial to in vivo conditions.. These studies suggest that *Col14a1* plays an important role in proliferation and growth of cardiomyocytes during later stages of myocardial maturation.

3.5 Cardiac fibroblast number is reduced in the post natal ventricular myocardium of *Col14a1*$^{-/-}$ mice

Our analyses show that in the absence of Collagen XIV, mRNA levels of differential collagens and matrix remodeling genes are significantly altered and myocyte proliferation is prolonged in the post natal myocardium. As previous studies have shown that cardiac fibroblasts interact with the ECM and cardiomyocytes to modulate homeostasis and remodeling of the myocardium [1], we examined this cell population in our system. At PND1, the percentage of cells expressing the fibroblast-associated marker Thy1, [30] was significantly lower in the post natal ventricular myocardium of *Col14a1*$^{-/-}$ mice (Figure 7A–C). In support, similar trends of reduced fibroblast numbers were also observed using a

second marker, Vimentin (7.1%±0.3 vs. 5.5%±0.2). These observations were consistent with a significant increase in the number of Thy1-positive cells co-expressing the apoptosis marker, Cleaved Caspase-3 (Figures 7D–F), however differences in Thy-1+ cell proliferation were not detected (Figure 7G–I). Therefore we conclude that cardiac fibroblast cell death is increased in Collagen XIV null mice at post natal stages.

3.6 Pressure overload enhances left ventricular wall growth in *Col14a1*$^{-/-}$ mice

Transverse aortic constriction (TAC) is commonly used as a model for pressure overload-induced cardiac hypertrophy [31]. In addition to myocyte enlargement (hypertrophy), animals subjected to TAC undergo extensive myocardial remodeling including an accumulation of interstitial collagen termed fibrosis, which is largely beneficial for ventricular remodeling short term, but long term, it increases ventricular stiffness, impairing cardiac function [32, 33]. To determine if hypertrophy and/or fibrosis is altered in *Col14a1*$^{-/-}$ mice, 8 week old null and *wild type* animals were subject to TAC to induce pressure overload for 2 weeks, or Sham surgery in which mice undergo the entire surgical procedure except for ligation of the aorta. As expected, compared to Sham mice, heart weight:body weight ratios, left ventricular posterior wall thickness (LVPW) and corrected left ventricular corrected mass were all increased in both *wild type* and *Col14a1*$^{-/-}$ mice subject to TAC (Table 1, Figure 8A–H). Interestingly, by determining the percent change of echocardiographic measurements between pre-versus post-surgery of Sham and TAC-operated mice, greater changes in LVPW and LV corrected mass were observed in *Col14a1*$^{-/-}$ mice following TAC, compared to *wild types* (Table 1). However, the average increase in myocyte cell size was not significantly different between genotypes after TAC, with an average increase of 37.71%±5.24 in *wild types* and 44.48%±5.02 in *Col14a1*$^{-/-}$ mice (p=0.4) (data not shown). At the level of fibrosis, Masson's Trichrome staining to detect collagen deposition revealed no significant difference between Sham versus TAC-operated *wild type* mice and *Col14a1*$^{-/-}$ animals (Figure 8I). Collagen types I and III are predominant within pathological fibrotic lesions of the heart [34]. In our system, comparable fold change increases in *Col1a1* were seen in both *wild type* (2.5±0.23) and *Col14a1*$^{-/-}$ (2.3±0.1) TAC-operated animals compared to respective Sham *wild types*, however the fold change of *Col3a1* expression was more significantly increased in *Col14a1*$^{-/-}$ (4.0±0.05) TAC- versus Sham-operated *Col14a1*$^{-/-}$ mice compared to *wild types* (2.4±0.24) (Figure 8J). Collectively, these studies suggest that increased left ventricular wall thickness is greater in *Col14a1*$^{-/-}$ subject to pressure overload compared to *wild type* animals, despite levels of cardiomyocyte hypertrophy and fibrotic responses being comparable.

4. Discussion

Collagen XIV is a FACIT-type collagen expressed in tissues of high mechanical stress [11–15]. Previously Ansorge et al., [11] generated mice null for this collagen type and reported dysfunctional fibrillogenesis in tendons and skin of mutant animals. In this current study, we report cardiac phenotypes and identify previously unappreciated roles for Collagen XIV in the development of the working myocardium. We observe that in the absence of Collagen XIV, the overall homeostasis of the ECM scaffold within the ventricular myocardium is compromised from as early as E11.5 (Figures 4 and 5) and associated with prolonged cardiomyocyte proliferation after birth and decreased myocyte size in adult *Col14a1*$^{-/-}$ mice (Figure 6). In addition, fewer fibroblasts within the ventricular myocardium are noted after birth as a result of increased apoptosis (Figure 7). These molecular and cellular abnormalities in young animals have detrimental effects on the overall structure and function of the adult working myocardium including exacerbated thickening of the left ventricular wall following pressure overload (Figure 8). These observations are one of the first to use a genetic mouse model to describe the importance of different collagens within

the cardiac interstitium for myocardial growth and maturation, therefore providing new insights into potential mechanisms of adult myocardial disease in the human population.

The composition of ECM is a major factor well studied in the adult heart [1], however relatively less is known about how the cardiac interstitium is assembled in the developing embryo [35]. In this study, we show that by E11.5, mRNA levels of many collagen types are highly expressed in the developing ventricular myocardium, predominantly fibril-forming types *Col1, Col2* and *Col3,* and comparable mRNA levels of the FACIT member, *Col14a1* (Figure 4). Spatially, Col14a1 is first observed in nonmyocardial structures including the endocardial cushions from as early as E10.5, and high levels of expression are maintained in adult valves (Figure 1C) [20]. Surprisingly, loss of *Col14a1* did not result in overt valvular phenotypes, suggesting a less important role in these connective tissue structures. In the myocardium, Collagen XIV immunoreactivity is not observed until E14.5, where it is localized to the subepicardial space and compact zone (Figure 1). Consistent with high levels of *Col14a1* mRNA at E11.5, null mice display dramatic changes in transcript levels of other collagen types in the ventricular myocardium at this time (Figure 4). This includes significant increases in fibril-forming collagens *Col1a1, Col1a2, Col3a1* and *Col27a1* that form the structural framework of the cardiac interstitium and provide tensile strength during high mechanical demand [1]. These observed alterations in collagen mRNA homeostasis at E11.5 suggests that similar to tendons, Collagen XIV plays a role in establishing the collagen network in the ventricular myocardium and observed increases in the closely related FACIT, *Col12a1* are not sufficient to compensate. It is known from Ansorge et al., [11] that Collagen XIV is important for fibrillogenesis, however it is appreciated that changes in transcript levels observed in this myocardial study may not reflect fibril assembly and fiber formation, although Collagen I protein levels were consistent with mRNA observations. Nonetheless, the lack of collagen fiber organization seen in the myocardium of *Col14a1*$^{-/-}$ mice (Figure 5C, D) along with significant changes in MMPs and their inhibitors, does suggest that assembly and remodeling of the cardiac interstititum is attenuated in this model. In contrast to tendons, these disruptions in collagen homeostasis do not affect the biomechanical properties of isolated ventricular skinned papillary fibers (Figure 3F). However, echocardiography to determine function of the intact heart indicates mild dilation of the left ventricle in the absence of hypertrophy, and decreased ejection fraction (Figure 3), although these parameters do not worsen after pressure overload. These studies suggest that defects in establishing the cardiac interstitium during development lead to attenuated physiological function of the working myocardium after birth. Additional studies using conditional approaches to delete *Col14a1* function after birth would further test this hypothesis and determine the requirement of Collagen XIV in the adult myocardium for maintaining structure-function relationships.

In addition to the ECM architecture, collagens are critical components of the development and maintenance of cellular organization, communication and function including cell survival [1]. In many systems, collagens have been shown to play roles in positively and negatively regulating cell proliferation and apoptosis [36–39], although to date, little is known about the embryonic heart. During early stages of myocardial development myocyte proliferation is rapid, however after birth, cell division is rarely observed and growth into adulthood relies on hypertrophy [40]. At E11.5, cardiomyocyte proliferation in *Col14a1*$^{-/-}$ embryos is apparently normal, yet at post natal stages proliferation rates are much higher than *wild types* (Figure 7A–C), suggesting that Collagen XIV is not required for promoting early cardiomyocyte cell proliferation, but potentially important for cell cycle withdrawal after birth. By three months of age, proliferation as expected, is virtually absent in both *wild types* and null animals, however due to differences at post natal stages, cardiomyocyte number is higher in ventricles of adult *Col14a1*$^{-/-}$ mice (Figure 7D–F). Interestingly, this hyperplastic phenotype does not lead to increased wall thickness at baseline, as determined

by echocardiography (Figure 3D), and this is likely due to the observed decrease in cardiomyocyte size in the absence of Collagen XIV. The mechanisms of prolonged proliferation in the post natal heart of *Col14a1*$^{-/-}$ mice are not clear and previous studies have reported a positive role for fibroblasts in promoting proliferation of embryonic myocytes [41, 42]. In the myocardium of *Col14a1*$^{-/-}$ mice fibroblast number is decreased as a result of apoptosis (Figure 7C), therefore suggesting that increased myocyte cell number is not due to expansion of the fibroblast cell population. However, it is considered that these opposing changes in myocyte and fibroblast cell survival in the neonatal myocardium of *Col14a1*$^{-/-}$ mice commonly stem from interruptions in formation of the collagen network during development. The effects of this will likely be detrimental on cell-cell and cell-ECM interactions [41], and lead to aberrations in known mechanisms of collagen-mediated cell survival, including integrin-mediated regulation of downstream signaling cascades such as PI3K/AKT [43–45]. Although these collective changes in myocardial cell number and size do not lead to hypertrophy or overt functional defects in adult *Col14a1*$^{-/-}$ mice at baseline, the pathological thickening of the left ventricular wall after TAC surgery is significantly greater than comparable surgeries in *wild type* mice (Figure 8, Table 1). As the degree of hypertrophy of individual myocytes in null animals is not significantly different, this suggests that in pressure overload conditions the underlying increase in myocyte number significantly promotes exacerbated pathological growth of the heart. This model of *Col14a1* deficiency provides insights into the importance of establishing the cardiac interstitium for the regulation of cardiomyocyte and fibroblast cell survival and therefore, susceptibility of the working myocardium after birth.

It is well established that collagens serve to positively regulate tissue morphogenesis and function, and defects in the assembly, organization and maintenance of collagen fibrils underlies and promotes the progression of many pathological states. In the adult heart this is most well understood during fibrosis when initial collagen deposition is considered beneficial for replacing interstitial regions occupied by necrotic myocytes, while long-term, collagen secretion becomes deleterious to the overall biomechanics and function of the heart [5]. Despite a striking alteration in the balance of collagen mRNA levels in *Col14a1*$^{-/-}$ mice from E11.5, as well as reduced fibroblast number at birth, the cardiac fibrosis program is not significantly affected two weeks after pressure overload. However, long-term evaluations of fibrous scar tissue formation and ventricular function were not made in *Col14a1*$^{-/-}$ mice in this current study. In the human population, collagen gene mutations underlie many connective tissue diseases including Ehlers-Danlos and Stickler Syndrome, and although musculoskeletal abnormalities are prominent in these patients, cardiac defects are not commonly reported [46]. However in this current mouse model, exacerbated pathological left ventricular wall thickening was only evident following pressure overload, and therefore it is considered that *Col14a1* loss of function may increase susceptibility in response to cardiac stress. To date, *COL14* mutations have not been identified in the human population and although *Col14a1*$^{-/-}$ mice are viable, several connective tissues associated with high mechanical demand (tendon, skin, myocardium) display structural abnormalities and functional weaknesses stemming from defects in collagen composition and organization. This current mouse model [11] is the first to demonstrate the role of FACIT collagens in formation of the cardiac interstitium within the developing myocardium, and the importance of Collagen XIV in regulating cardiomyocyte and fibroblast cell populations during post natal stages. Further, we demonstrate that aberrations in assembly of the collagen network during embryonic development have detrimental effects on cardiac structure function after birth, particularly in a pressure overload model. Identification of the mechanism(s) underlying development of healthy myocardium will provide valuable insights into the mechanisms of cardiac disease including the previously unappreciated susceptibility in patients with connective tissue disorders.

Acknowledgments

We thank Shelia Adams, Blair Austin, Damien Barnette, Harriet Hammond and Jingsheng Liang for technical assistance, in addition to Dr. Vidu Garg for scientific discussion. This work was supported by NIH/NHLBI (HL091878, JL) and AHA Predoctoral Fellowship (10PRE4360052, GT).

References

1. Bowers SL, Banerjee I, Baudino TA. The extracellular matrix: at the center of it all. J Mol Cell Cardiol. 2010; 48:474–482. [PubMed: 19729019]
2. Eghbali M, Weber KT. Collagen and the myocardium: fibrillar structure, biosynthesis and degradation in relation to hypertrophy and its regression. Molecular and cellular biochemistry. 1990; 96:1–14. [PubMed: 2146489]
3. Lockhart M, Wirrig E, Phelps A, Wessels A. Extracellular matrix and heart development. Birth Defects Res A Clin Mol Teratol. 2011; 91:535–550. [PubMed: 21618406]
4. Carver W, Terracio L, Borg TK. Expression and accumulation of interstitial collagen in the neonatal rat heart. Anat Rec. 1993; 236:511–520. [PubMed: 8363055]
5. Jourdan-Lesaux C, Zhang J, Lindsey ML. Extracellular matrix roles during cardiac repair. Life Sci. 2010; 87:391–400. [PubMed: 20670633]
6. Zhang G, Young BB, Ezura Y, Favata M, Soslowsky LJ, Chakravarti S, et al. Development of tendon structure and function: regulation of collagen fibrillogenesis. Journal of musculoskeletal & neuronal interactions. 2005; 5:5–21. [PubMed: 15788867]
7. Iozzo RV. Matrix proteoglycans: from molecular design to cellular function. Annual review of biochemistry. 1998; 67:609–652.
8. Birk DE, Lande MA. Corneal and scleral collagen fiber formation in vitro. Biochimica et biophysica acta. 1981; 670:362–369. [PubMed: 7295781]
9. Rada JA, Cornuet PK, Hassell JR. Regulation of corneal collagen fibrillogenesis in vitro by corneal proteoglycan (lumican and decorin) core proteins. Experimental eye research. 1993; 56:635–648. [PubMed: 8595806]
10. Pogany G, Vogel KG. The interaction of decorin core protein fragments with type I collagen. Biochemical and biophysical research communications. 1992; 189:165–172. [PubMed: 1449470]
11. Ansorge HL, Meng X, Zhang G, Veit G, Sun M, Klement JF, et al. Type XIV Collagen Regulates Fibrillogenesis: PREMATURE COLLAGEN FIBRIL GROWTH AND TISSUE DYSFUNCTION IN NULL MICE. J Biol Chem. 2009; 284:8427–8438. [PubMed: 19136672]
12. Walchli C, Koch M, Chiquet M, Odermatt BF, Trueb B. Tissue-specific expression of the fibril-associated collagens XII and XIV. J Cell Sci. 1994; 107(Pt 2):669–681. [PubMed: 8207089]
13. Berthod F, Germain L, Guignard R, Lethias C, Garrone R, Damour O, et al. Differential expression of collagens XII and XIV in human skin and in reconstructed skin. J Invest Dermatol. 1997; 108:737–742. [PubMed: 9129225]
14. Niyibizi C, Visconti CS, Kavalkovich K, Woo SL. Collagens in an adult bovine medial collateral ligament: immunofluorescence localization by confocal microscopy reveals that type XIV collagen predominates at the ligament-bone junction. Matrix Biol. 1995; 14:743–751. [PubMed: 8785589]
15. Young BB, Gordon MK, Birk DE. Expression of type XIV collagen in developing chicken tendons: association with assembly and growth of collagen fibrils. Dev Dyn. 2000; 217:430–439. [PubMed: 10767087]
16. Gerecke DR, Meng X, Liu B, Birk DE. Complete primary structure and genomic organization of the mouse Col14a1 gene. Matrix Biol. 2004; 22:595–601. [PubMed: 15065570]
17. Rasi K, Hurskainen M, Kallio M, Staven S, Sormunen R, Heape AM, et al. Lack of collagen XV impairs peripheral nerve maturation and, when combined with laminin-411 deficiency, leads to basement membrane abnormalities and sensorimotor dysfunction. J Neurosci. 2010; 30:14490–14501. [PubMed: 20980607]
18. Lincoln J, Florer JB, Deutsch GH, Wenstrup RJ, Yutzey KE. ColVa1 and ColXIa1 are required for myocardial morphogenesis and heart valve development. Dev Dyn. 2006; 235:3295–3305. [PubMed: 17029294]

19. Levay AK, Peacock JD, Lu Y, Koch M, Hinton RB Jr, Kadler KE, et al. Scleraxis is required for cell lineage differentiation and extracellular matrix remodeling during murine heart valve formation in vivo. Circ Res. 2008; 103:948–956. [PubMed: 18802027]
20. Peacock JD, Lu Y, Koch M, Kadler KE, Lincoln J. Temporal and spatial expression of collagens during murine atrioventricular heart valve development and maintenance. Dev Dyn. 2008; 237:3051–3058. [PubMed: 18816857]
21. Peacock JD, Levay AK, Gillaspie DB, Tao G, Lincoln J. Reduced sox9 function promotes heart valve calcification phenotypes in vivo. Circ Res. 2010; 106:712–719. [PubMed: 20056916]
22. Veit G, Hansen U, Keene DR, Bruckner P, Chiquet-Ehrismann R, Chiquet M, et al. Collagen XII interacts with avian tenascin-X through its NC3 domain. J Biol Chem. 2006; 281:27461–27470. [PubMed: 16861231]
23. Birk DE, Trelstad RL. Extracellular compartments in tendon morphogenesis: collagen fibril, bundle, and macroaggregate formation. J Cell Biol. 1986; 103:231–240. [PubMed: 3722266]
24. Lincoln J, Kist R, Scherer G, Yutzey KE. Sox9 is required for precursor cell expansion and extracellular matrix organization during mouse heart valve development. Developmental biology. 2007; 305:120–132. [PubMed: 17350610]
25. Baudenbacher F, Schober T, Pinto JR, Sidorov VY, Hilliard F, Solaro RJ, et al. Myofilament Ca2+ sensitization causes susceptibility to cardiac arrhythmia in mice. J Clin Invest. 2008; 118:3893–3903. [PubMed: 19033660]
26. Wilkins BJ, Dai YS, Bueno OF, Parsons SA, Xu J, Plank DM, et al. Calcineurin/NFAT coupling participates in pathological, but not physiological, cardiac hypertrophy. Circ Res. 2004; 94:110–118. [PubMed: 14656927]
27. Shenouda SK, Lord KC, McIlwain E, Lucchesi PA, Varner KJ. Ecstasy produces left ventricular dysfunction and oxidative stress in rats. Cardiovasc Res. 2008; 79:662–670. [PubMed: 18495670]
28. Levick SP, Brower GL. Regulation of matrix metalloproteinases is at the heart of myocardial remodeling. Am J Physiol Heart Circ Physiol. 2008; 295:H1375–H1376. [PubMed: 18757475]
29. Clark IM, Swingler TE, Sampieri CL, Edwards DR. The regulation of matrix metalloproteinases and their inhibitors. Int J Biochem Cell Biol. 2008; 40:1362–1378. [PubMed: 18258475]
30. Hudon-David F, Bouzeghrane F, Couture P, Thibault G. Thy-1 expression by cardiac fibroblasts: lack of association with myofibroblast contractile markers. J Mol Cell Cardiol. 2007; 42:991–1000. [PubMed: 17395197]
31. deAlmeida AC, van Oort RJ, Wehrens XH. Transverse aortic constriction in mice. J Vis Exp. 2010
32. Creemers EE, Pinto YM. Molecular mechanisms that control interstitial fibrosis in the pressure-overloaded heart. Cardiovasc Res. 2011; 89:265–272. [PubMed: 20880837]
33. Oka T, Xu J, Kaiser RA, Melendez J, Hambleton M, Sargent MA, et al. Genetic manipulation of periostin expression reveals a role in cardiac hypertrophy and ventricular remodeling. Circ Res. 2007; 101:313–321. [PubMed: 17569887]
34. van den Borne SW, Diez J, Blankesteijn WM, Verjans J, Hofstra L, Narula J. Myocardial remodeling after infarction: the role of myofibroblasts. Nat Rev Cardiol. 2010; 7:30–37. [PubMed: 19949426]
35. Espira L, Czubryt MP. Emerging concepts in cardiac matrix biology. Can J Physiol Pharmacol. 2009; 87:996–1008. [PubMed: 20029536]
36. Sasaki J, Fujisaki H, Adachi E, Irie S, Hattori S. Delay of cell cycle progression and induction death of cancer cells on type I collagen fibrils [corrected]. Connective tissue research. 2011; 52:167–177. [PubMed: 20672981]
37. Hopfer U, Hopfer H, Meyer-Schwesinger C, Loeffler I, Fukai N, Olsen BR, et al. Lack of type VIII collagen in mice ameliorates diabetic nephropathy. Diabetes. 2009; 58:1672–1681. [PubMed: 19401424]
38. Ieda M, Tsuchihashi T, Ivey KN, Ross RS, Hong TT, Shaw RM, et al. Cardiac fibroblasts regulate myocardial proliferation through beta1 integrin signaling. Developmental cell. 2009; 16:233–244. [PubMed: 19217425]
39. Cheng IH, Lin YC, Hwang E, Huang HT, Chang WH, Liu YL, et al. Collagen VI protects against neuronal apoptosis elicited by ultraviolet irradiation via an Akt/phosphatidylinositol 3-kinase signaling pathway. Neuroscience. 2011; 183:178–188. [PubMed: 21459131]

40. Ahuja P, Sdek P, MacLellan WR. Cardiac myocyte cell cycle control in development, disease, and regeneration. Physiological reviews. 2007; 87:521–544. [PubMed: 17429040]

41. Baudino TA, Carver W, Giles W, Borg TK. Cardiac fibroblasts: friend or foe? Am J Physiol Heart Circ Physiol. 2006; 291:H1015–H1026. [PubMed: 16617141]

42. Ieda M, Fukuda K. Cardiac innervation and sudden cardiac death. Current cardiology reviews. 2009; 5:289–295. [PubMed: 21037846]

43. Howell SJ, Doane KJ. Type VI collagen increases cell survival and prevents anti-beta 1 integrin-mediated apoptosis. Experimental cell research. 1998; 241:230–241. [PubMed: 9633532]

44. Milner R, Campbell IL. The integrin family of cell adhesion molecules has multiple functions within the CNS. Journal of neuroscience research. 2002; 69:286–291. [PubMed: 12125070]

45. Iyengar P, Espina V, Williams TW, Lin Y, Berry D, Jelicks LA, et al. Adipocyte-derived collagen VI affects early mammary tumor progression in vivo, demonstrating a critical interaction in the tumor/stroma microenvironment. J Clin Invest. 2005; 115:1163–1176. [PubMed: 15841211]

46. Malfait F, Wenstrup RJ, De Paepe A. Clinical and genetic aspects of Ehlers-Danlos syndrome, classic type. Genetics in medicine : official journal of the American College of Medical Genetics. 2010; 12:597–605. [PubMed: 20847697]

Highlights

- Collagen XIV is expressed in the developing and mature heart
- *Col14a1*$^{-/-}$ mice have alterations in collagen homeostasis and organization
- *Col14a1* regulates cardiomyocyte proliferation and fibroblast apoptosis
- Cardiac stress increased myocardial wall thickening in *Col14a1*$^{-/-}$ mice

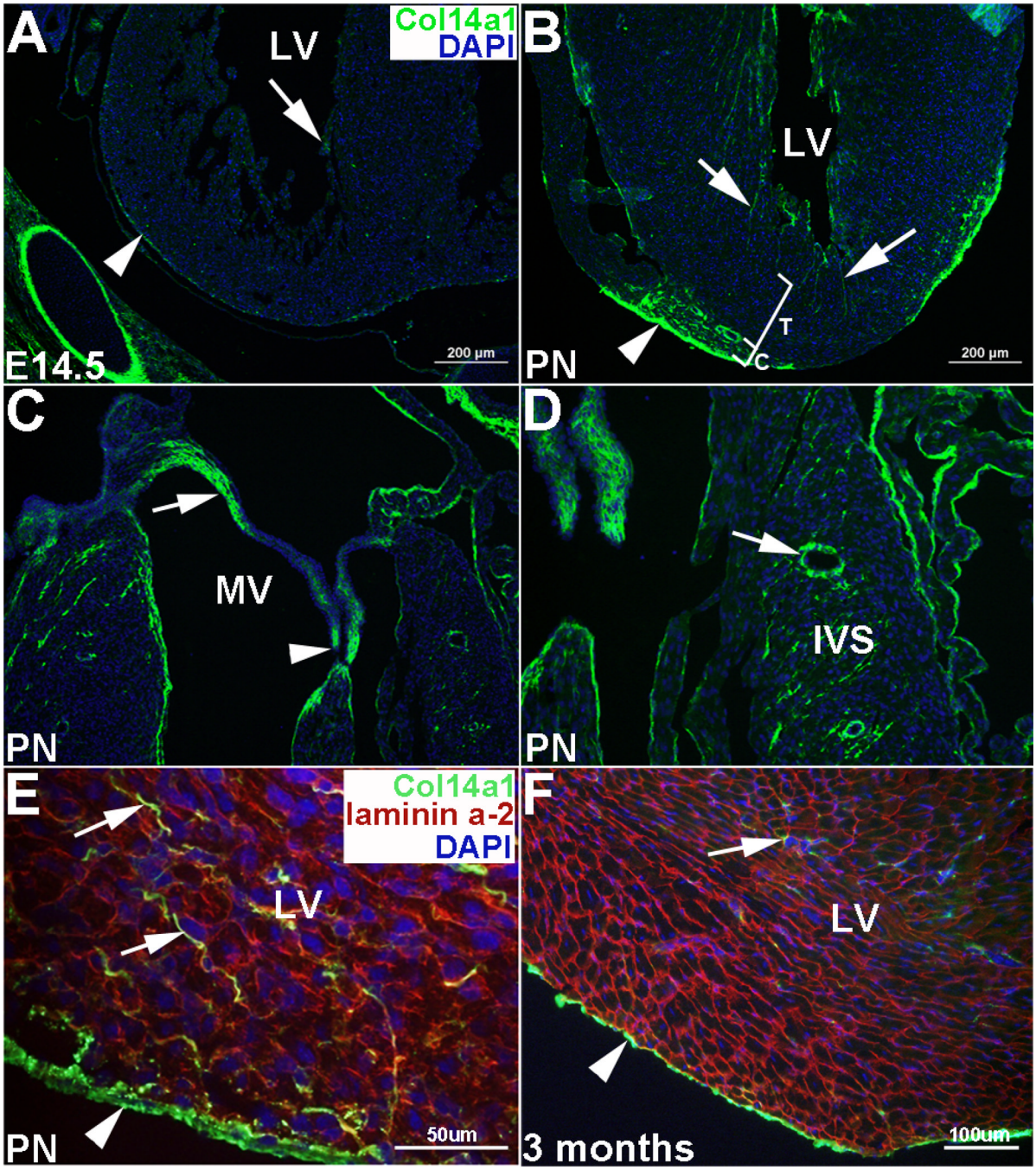

Figure 1. Collagen XIV is expressed in embryonic and adult mouse hearts

(A) Immunofluorescence to show Collagen XIV expression at low levels within the cardiac interstitium of the developing murine myocardium at E14.5 (arrows), and subepicardial region (arrowhead). (B–E) Collagen XIV immunoreactivity is more highly expressed in the myocardium at post natal (PN) stages, with comparatively stronger immunoreactivity within the compact (C) versus trabeculae (T) layers, and continued high expression in the subepicardial region (arrowhead). (C) At PN stages, expression is also detected in the leaflets (arrow) and chordae tendineae (arrowhead) of the valves (mitral valve shown), as well as the intramyocardial coronary vessels (arrow, D). (E) Higher magnification of Collagen XIV immunoreactivity within the cardiac interstitium of the PN heart (arrows).

Laminin α2 indicates cell membranes and DAPI, nuclei. (F) By 3 months of age, Collagen XIV is still detectable within the adult myocardium, although levels are reduced. LV, left ventricle; IVS, interventricular septum; MV, mitral valve, PN, post natal.

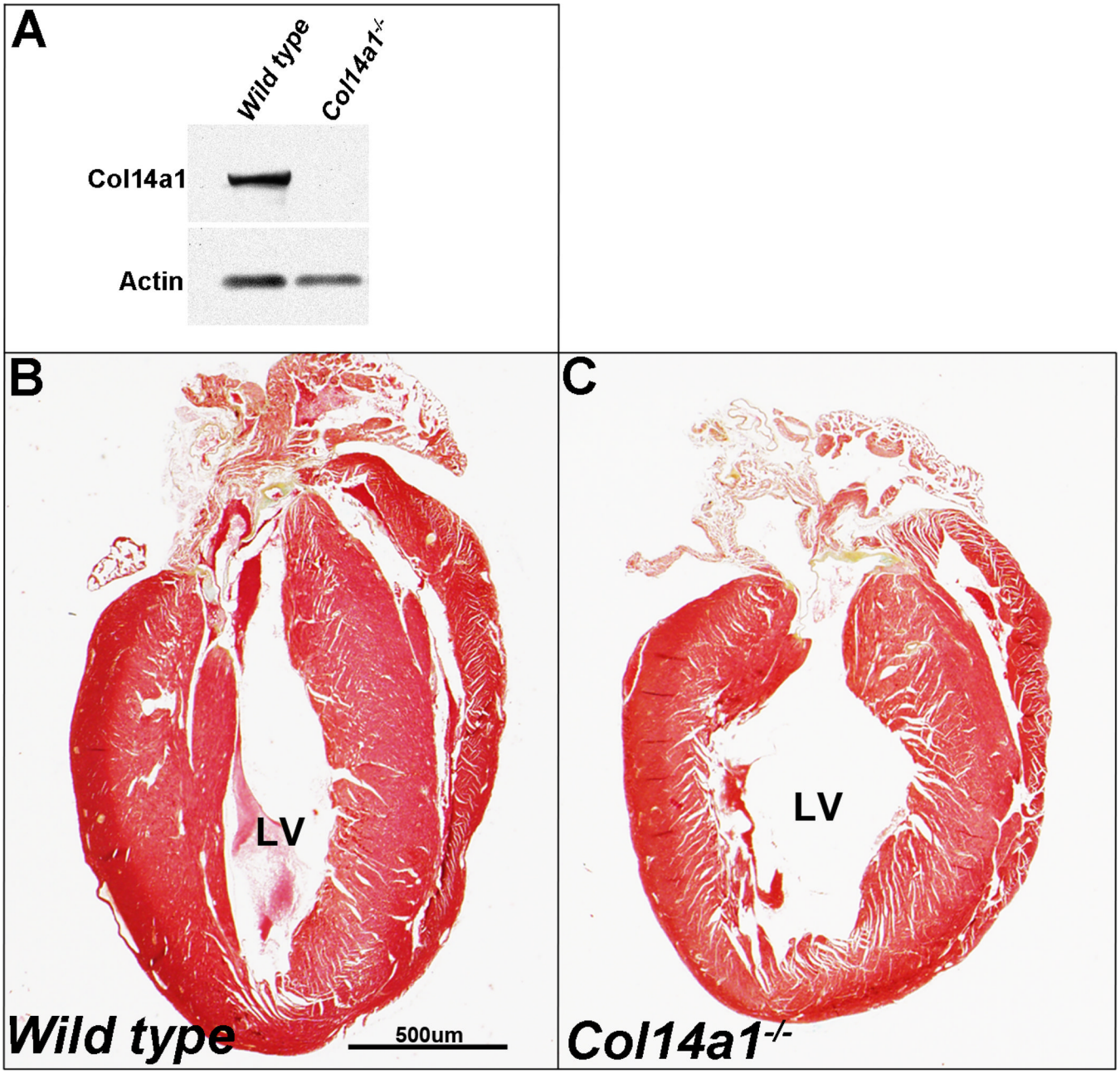

Figure 2. *Col14a1*$^{-/-}$ mice show gross histological changes in ventricular morphology at 3 months of age

(A) Western blot of Collagen XIV expression in collagen extracts from post natal *wild type* (*Col14a1*$^{+/+}$), and *Col14a1*$^{-/-}$ hearts. Note loss of protein in *Col14a1*$^{-/-}$ mice. Actin is used as a loading control. (B, C) Pentachrome staining to show cardiac morphology of 3 month old *wild type* (B) and *Col14a1*$^{-/-}$ (C) mouse hearts. Note the spherical appearance of the left ventricle of *Col14a1*$^{-/-}$ hearts. LV, left ventricle.

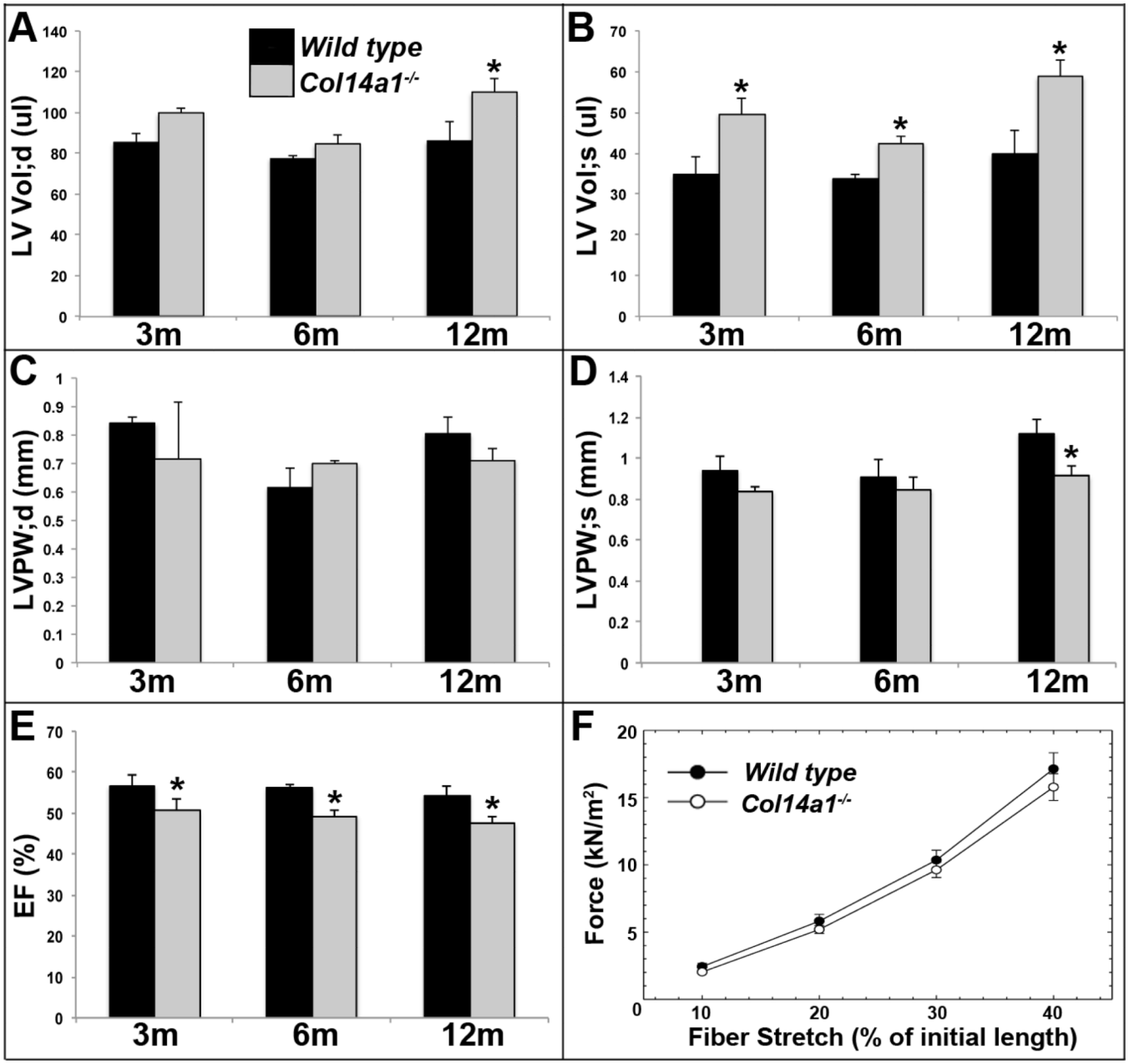

Figure 3. Echocardiography reveals differences in cardiac structure and function in adult *Col14a1*$^{-/-}$ male mice

M-mode Doppler analysis to show left ventricular end-diastolic volume (LV vol;d) (A), LV end-systolic volume during systole (LV vol;s) (B), LV posterior wall thickness (LVPW) during diastole (d) (C), LVPW during systole (s) (D), and ejection fraction (EF) in *Col14a1*$^{-/-}$ and *Col14a1*$^{+/+}$ male mice at 3, 6, and 12 months of age. *, indicates statistical significance, $p<0.05$. (F) Stretch-force relationship assay to determine maximal stretch of skinned fibers from 3 month old *Col14a1*$^{-/-}$ and *wild type* mice.

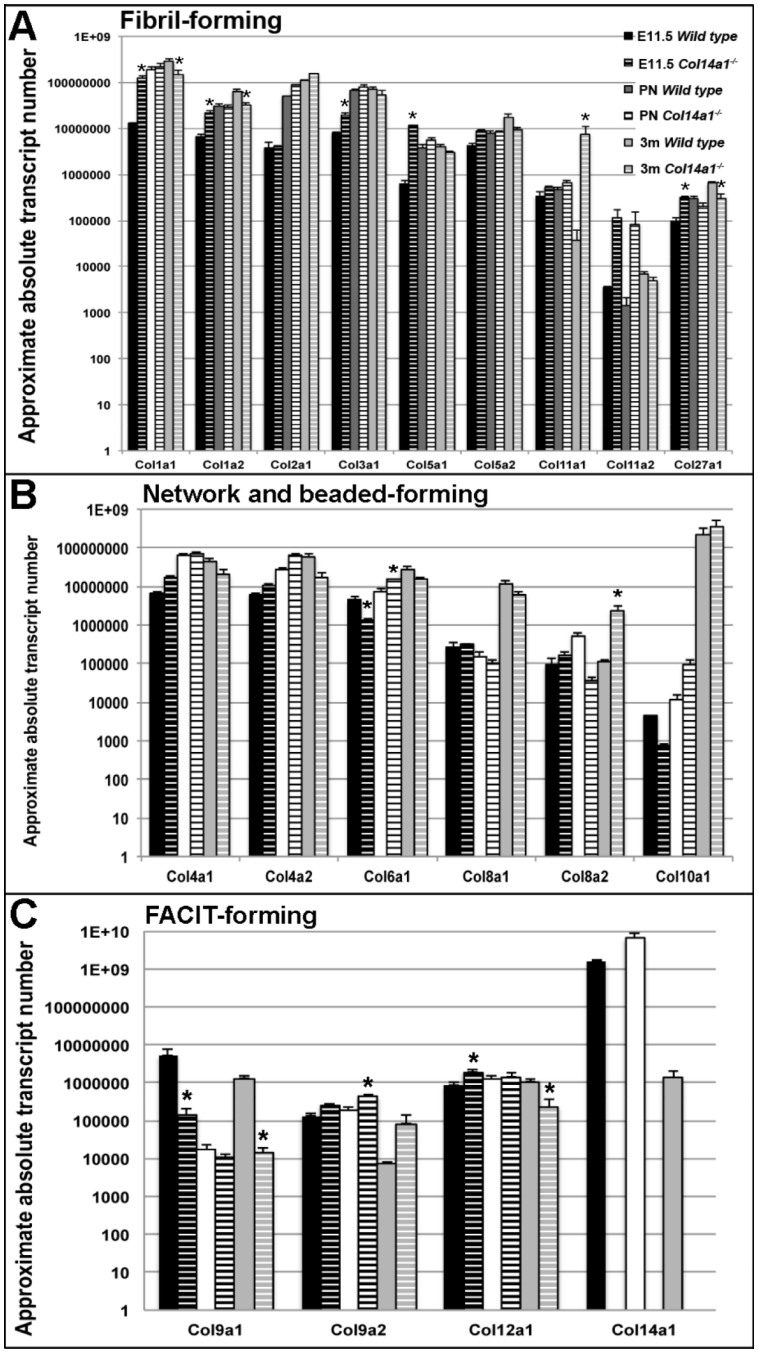

Figure 4. Collagen homeostasis is disrupted in the myocardium of *Col14a1*$^{-/-}$ mice

Taqman Low Density Array was used to examine changes in mRNA levels of fibril-forming (A), network and beaded-forming (B) and FACIT-forming (C) collagens in cDNA generated from E11.5, PND1 and 3 months *Col14a1*$^{-/-}$ and *Col14a1*$^{+/+}$ (*wild type*) ventricles. *, indicate $p<0.05$ in samples from *Col14a1*$^{-/-}$ mice compared to *wild types*.

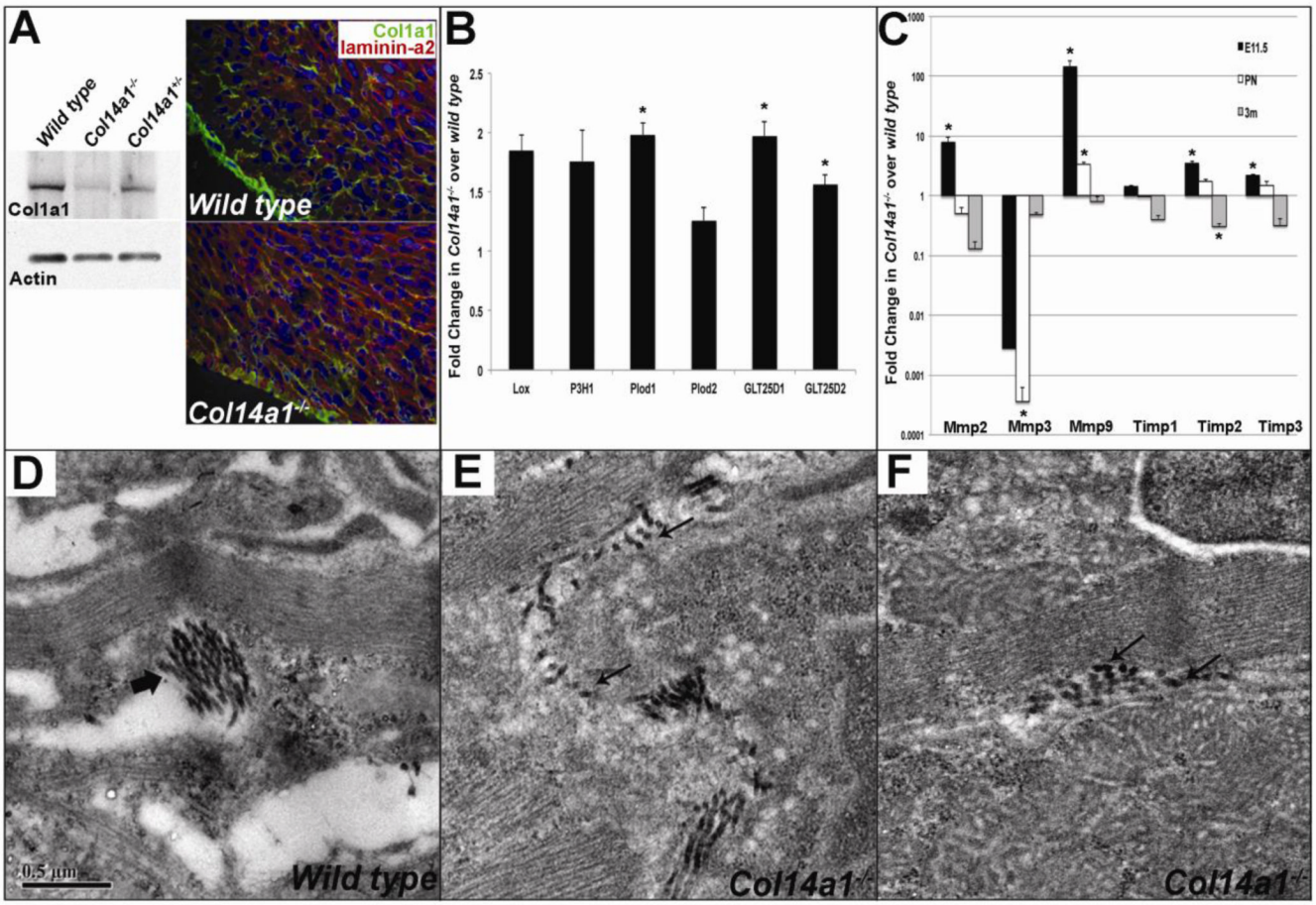

Figure 5. Collagen fiber organization and remodeling gene expression is altered in the myocardium of *Col14a1*$^{-/-}$ mice

(A) Western blot (left) and immunofluorescence (right) to show decreased Col1a1 expression in the ventricular myocardium of 3 month old *Col14a1*$^{-/-}$, *Col14a1*$^{+/-}$ and *wild type* mice. (B) qPCR analysis to show fold changes in collagen processing enzymes in the ventricular myocardium of post natal *Col14a1*$^{-/-}$ compared to *wild type* controls. (C) TLDA analysis to show fold changes in expression of matrix remodeling genes in the ventricular myocardium of *Col14a1*$^{-/-}$ mice at E11.5, PN and 3 months of age. (D–F) Electron microscopy to examine collagen fiber organization in the ventricular myocardium of *wild type* (D) and *Col14a1*$^{-/-}$ mice (E–F) at PND1. Note lack of collagen fiber bundles in *Col14a1*$^{-/-}$ mice (E–F), compared to *wild types* (arrow, D).

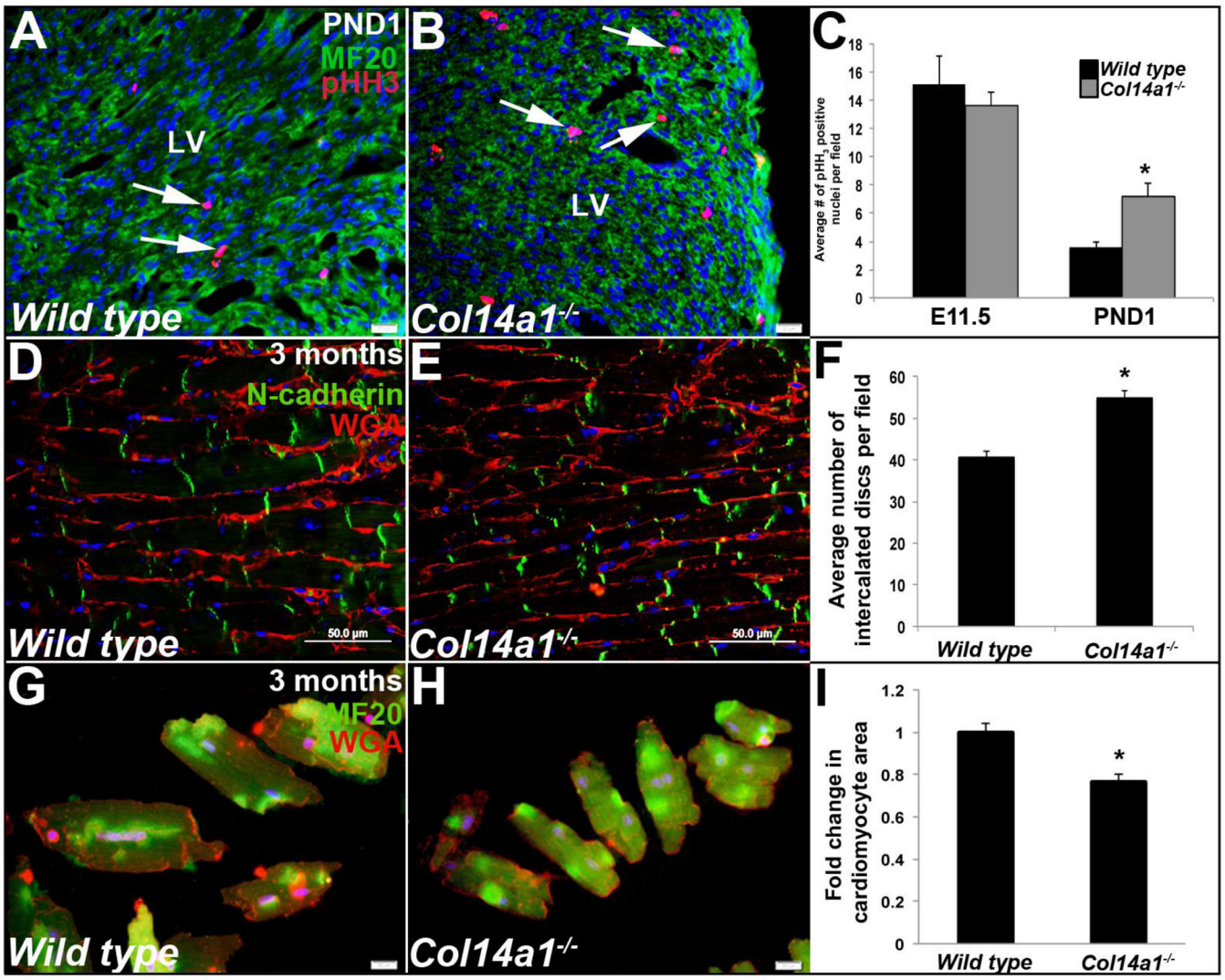

Figure 6. Cardiomyocyte proliferation is prolonged in the myocardium of *Col14a1*$^{-/-}$ mice at post natal stages

(A–C) Immunostaining of phospho-Histone H3 (pHH3) and MF20 to examine proliferation of cardiomyocytes respectively in PND1 *Col14a1*$^{-/-}$ mice (B) and *wild types* (A). Quantitation of the number of cells double stained with MF20 and pHH3 at E11.5 and PND1. (D, E) Immunoreactivity of N-cadherin to detect intercalated discs of cardiomyocytes in tissue sections of ventricles from 3 month old *Col14a1*$^{-/-}$ (E) and *wild type* (D) mice. Wheat Germ Agglutinin (WGA) highlights the cell membrane, and DAPI indicates nuclei. (F) Quantitation of the average number of cells per microscopic field. (G, H) MF20 immunostaining of cultured ventricular cardiomyocytes isolated from 3 month old *Col14a1*$^{-/-}$ (H) and *wild type* (G) mice. (I) Quantitation to show fold change in cardiomyocyte cell area. *p<0.05, in *Col14a1*$^{-/-}$ mice compared to *wild types*.

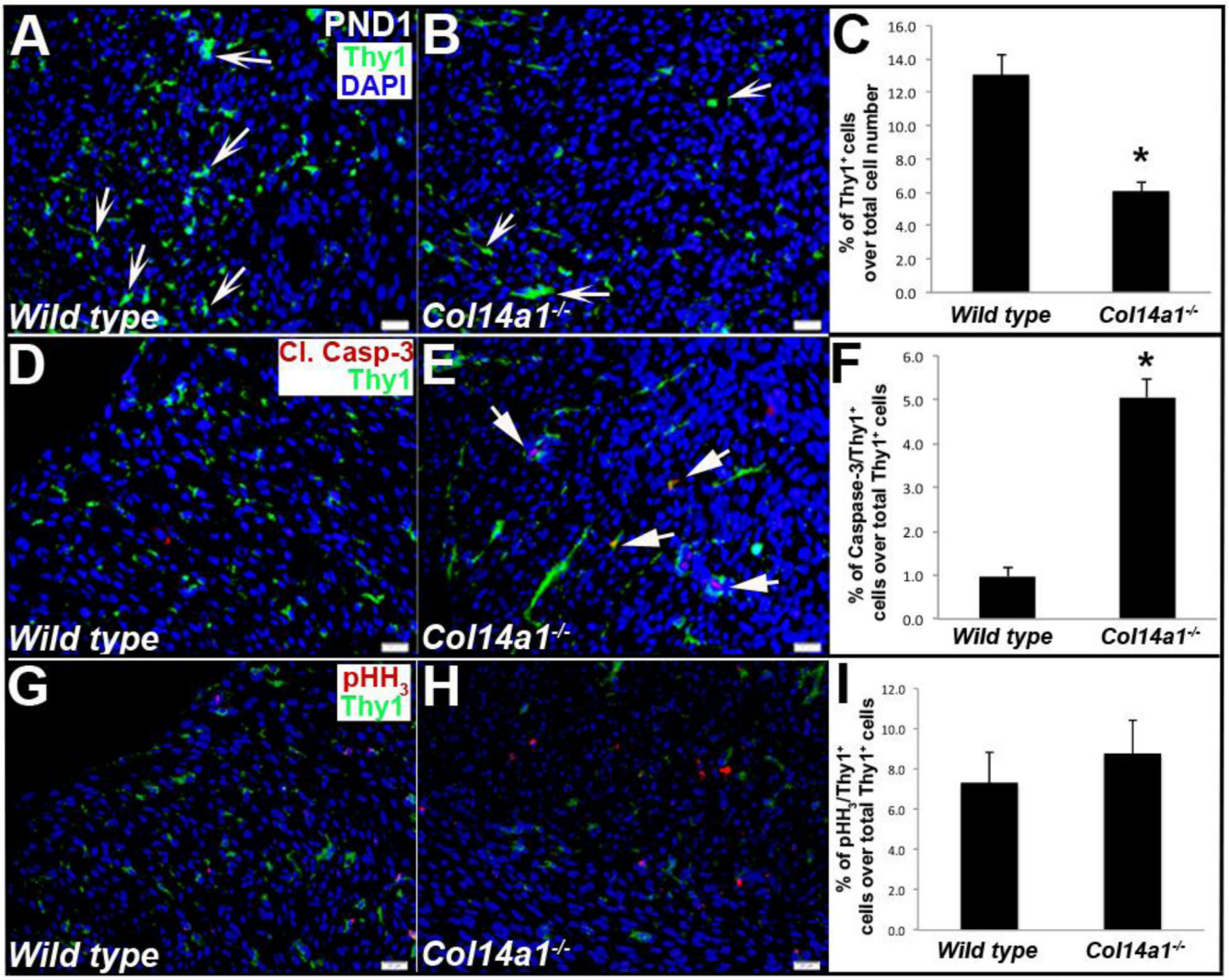

Figure 7. Fibroblast cell number is decreased in the ventricular myocardium of *Col14a1*$^{-/-}$ mice at post natal stages

(A, B) Thy1 immunostaining to detect cardiac fibroblasts (arrows) within the ventricular myocardium of *Col14a1*$^{-/-}$ (B) and *wild type* (*Col14a1*$^{-/-}$) mice (A) at PND1. (C) Percentage of Thy1 positive cells over the total number of nuclei. (D, E) Double immunostaining of Cleaved Caspase-3 and Thy1 within the ventricular myocardium of *Col14a1*$^{-/-}$ (E) and *wild type* (*Col14a1*$^{-/-}$) mice (D) at the same time point. Arrowhead in D indicates apoptosis in a non-fibroblast cell, while arrows in E indicate double stained fibroblasts undergoing apoptosis. (F) Percentage of double stained (Cleaved Caspase-3 and Thy1) cells in *Col14a1*$^{-/-}$ and *wild type* mice over total number of Thy1-positive cells. (G, H) Double staining of phospho-Histone H_3 (pHH_3) and Thy1 within the ventricular myocardium of *Col14a1*$^{-/-}$ (H) and *wild type* (H) mice. (I) Percentage of double stained (pHH_3 and Thy1) cells in *Col14a1*$^{-/-}$ and *wild type* mice over total number of Thy1-positive cells. *$p<0.05$, statistical significance in *Col14a1*$^{-/-}$mice compared to *wild types*.[13]

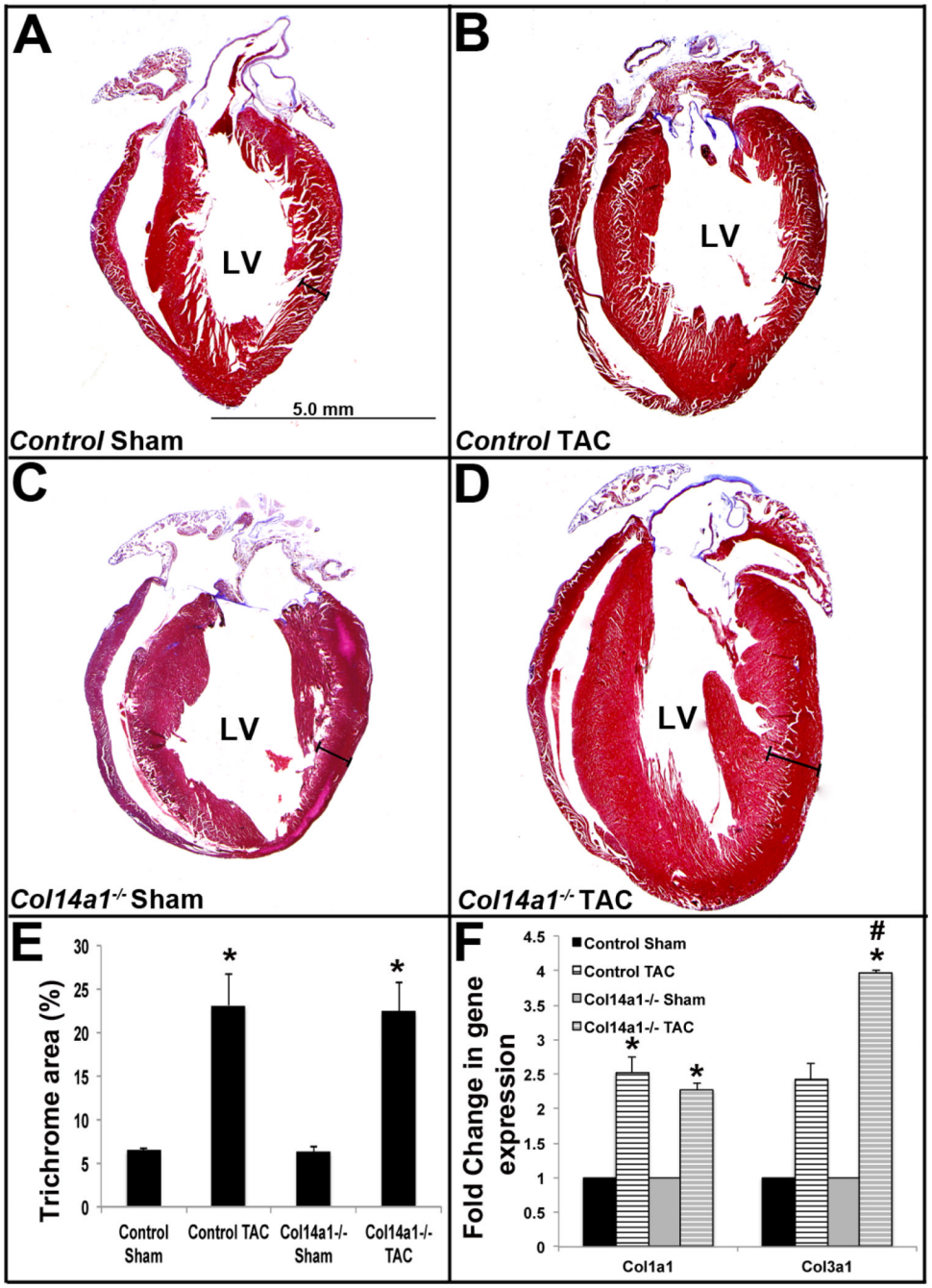

Figure 8. Left ventricular wall thickness is further increased in *Col14a1*$^{-/-}$ mice following pressure overload

(A–H) Images from echocardiography B-mode short-axis view of the ventricular chambers of *wild type* (A–D) and *Col14a1*$^{-/-}$ (E–H) mice, prior to surgery (pre-surgery) (A, C, E, G) and two weeks post-surgery (B, D, F, H). Red lines indicate left ventricular wall thickness. White * indicate papillary muscles in the shortaxis view. (I) Quantitation of trichrome staining and (J) qPCR of fold changes in *Col1a1* and *Col3a1* gene expression in the ventricles of *wild type* and *Col14a1*$^{-/-}$ mice following surgeries. *, indicates significant differences in TAC-operated animals versus Sham mice of the same genotype. #, shows

$p<0.05$ in differences between Sham and TAC in *Col14a1*$^{-/-}$ mice compared to differences observed between *wild types*.

J Mol Cell Cardiol. Author manuscript; available in PMC 2013 November 01.

Table 1

Echocardiography measurements of *wild type* and *Col14a1*$^{-/-}$ mice following Sham and TAC surgeries

Sham and TAC surgeries were performed on 8 week old *wild type* (*ca1*$^{+/+}$) and *Col14a1*$^{-/-}$ mice. (Top) Average measurements taken from four experimental groups subjected to echocardiography pre-surgery, and 2 weeks post-surgery. (Bottom) Average percent changes in echocardiographic measurements of individual *wild type* and *Col14a1*$^{-/-}$ mice subject to Sham and TAC, comparing pre-surgery vs. post-surgery.

	LVPW;d (mm)	LVPW;s (mm)	PWTH (%)	LVID stroke vol. (μl)	EF (%)	LV Mas corrected (mg)	HW/BW (mg/g)
Pre-surgery							
***Wild type* Sham**	0.64±0.09	0.83±0.13	29.36±2.26	40.63±5.95	52.90±6.17	76.59±8.87	
***Wild type* TAC**	0.65±0.04	0.84±0.04	28.82±13.75	42.36±3.25	52.13±6.91	78.60±10.14	
***Col14a1*$^{-/-}$ Sham**	0.72±0.03	0.87±0.07	21.59±13.61	43.38±9.63	49.27±6.02	93.77±18.68	
***Col14a1*$^{-/-}$ TAC**	0.66±0.05	0.82±0.09	23.68±11.48	40.90±8.19	46.08±5.15	84.66±14.64	
Post-surgery							
***Wild type* Sham**	0.64±0.12	0.78±0.16	21.06±5.05	37.88±3.63	52.62±5.24	82.58±20.07	0.64±0.12
***Wild type* TAC**	0.82±0.14	1.06±0.14	29.97±11.54	39.23±3.65	55.10±5.05	96.39±19.92	0.82±0.14*
***Col14a1*$^{-/-}$ Sham**	0.70±0.10	0.81±0.09	16.23±12.85	43.58±7.73	48.73±5.44	93.00±27.99	0.70±0.10
***Col14a1*$^{-/-}$ TAC**	0.88±0.10	1.05±0.11	20.47±12.26	42.57±11.77	47.22±10.49	111.64±15.59	0.88±0.10*§

% Change (Pre- vs. Post-surgery)	LVPW;d	LVPW;s	PWTH	LVID stroke vol.c	EF	LV Mass corrected
***Wild type* Sham**	0±5	−7±6	−28±20	−5±18	0±1	7±16
***Wild type* TAC**	20±8#	26±14#	1±21	−8±9	5±11	19±4
***Col14a1*$^{-/-}$ Sham**	−2±14	−7±7	−63±105	4±23	0±2	−1±16
***Col14a1*$^{-/-}$ TAC**	39±13*§	29±11§	−56±28*	4±35	4±8	35±7*§

Sham vs. TAC within the same genotype;

¶ Pre-surgery vs. post-surgery within the same genotype;

§ *Wild type* TAC vs. *Col14a1*$^{-/-}$ TAC (post surgery).

Note, no significant differences were observed between *Wild type* Sham vs. *Col14a1*$^{-/-}$ Sham post-surgery groups. Data presented as standard error of the ean. LVPW, Left ventricular wall thickness; LVID, left ventricular internal dimension; EF, Ejection fraction; Ao, aortic; LV, left ventricular; HW, heart weight; BW, body weight.